(2)

NRL Memorandum Report 5277

A Transmission Line Bridge for the Diagnostics of Plasma Channels

R. E. PECHACEK, M. RALEIGH, AND J. R. GREIG

Experimental Plasma Physics Branch
Plasma Physics Division

T. DWYER

U. S. Navy

J. EHRLICH

Sachs/Freeman Associates
Bowie, MD 20715

March 7, 1984

This research was supported by the Office of Naval Research and by the Defense Advanced Research Projects Agency (DoD) ARPA Order No. 4395, Amendment No. 11, monitored by the Naval Surface Weapons Center under Contract N60921-83-WR-W0014.

NAVAL RESEARCH LABORATORY
Washington, D.C.

SECURITY CLASSIFICATION OF THIS PAGE

REPORT DOCUMENTATION PAGE

1a. REPORT SECURITY CLASSIFICATION UNCLASSIFIED	1b. RESTRICTIVE MARKINGS
2a. SECURITY CLASSIFICATION AUTHORITY	3. DISTRIBUTION/AVAILABILITY OF REPORT Approved for public release; distribution unlimited.
2b. DECLASSIFICATION/DOWNGRADING SCHEDULE	
4. PERFORMING ORGANIZATION REPORT NUMBER(S) NRL Memorandum Report 5277	5. MONITORING ORGANIZATION REPORT NUMBER(S)
6a. NAME OF PERFORMING ORGANIZATION Naval Research Laboratory 6b. OFFICE SYMBOL (If applicable)	7a. NAME OF MONITORING ORGANIZATION Naval Surface Weapons Center
6c. ADDRESS (City, State and ZIP Code) Washington, DC 20375	7b. ADDRESS (City, State and ZIP Code) Silver Spring, MD 20910
8a. NAME OF FUNDING/SPONSORING ORGANIZATION ONR and DARPA 8b. OFFICE SYMBOL (If applicable)	9. PROCUREMENT INSTRUMENT IDENTIFICATION NUMBER
8c. ADDRESS (City, State and ZIP Code) Arlington, VA 22217 Arlington, VA 22209	10. SOURCE OF FUNDING NOS. PROGRAM ELEMENT NO.: 61153N / 62707E PROJECT NO.: TASK NO.: RR011-09-41 / OR [illegible] AA WORK UNIT NO.: 47-0871 / 47-0922
11. TITLE (Include Security Classification) (See page ii)	
12. PERSONAL AUTHOR(S) R. E. Pechacek, M. Raleigh, J. R. Greig, T. Dwyer,* and J. Ehrlich**	
13a. TYPE OF REPORT Interim 13b. TIME COVERED FROM _____ TO _____	14. DATE OF REPORT (Yr., Mo., Day) March 7, 1984 15. PAGE COUNT 26
16. SUPPLEMENTARY NOTATION *U. S. Navy **Sachs/Freeman Associates, Bowie, MD 20715 (Continues)	
17. COSATI CODES FIELD / GROUP / SUB. GR.	18. SUBJECT TERMS (Continue on reverse if necessary and identify by block number) Diagnostic Transmission line Plasma channels

19. ABSTRACT (Continue on reverse if necessary and identify by block number)

A transmission line bridge is a device for measuring the dielectric constant of long, narrow, plasma columns. The device measures the difference in propagation properties between a reference line and a line whose capacitance per unit length has been changed by the presence of ionization. The particular transmission line bridge described, consisting of two two-wire transmission lines, was operated at a frequency of 30 MHz. It was used to measure conductivities in the range of $10^3 < \sigma < 1.5 \times 10^6$ Hz for plasma columns in the atmosphere, $\sim$1 m long and $\sim$1 cm radius, created by laser induced breakdown. The lower limit on measurable conductivity is determined by system noise and is less than 10^3 Hz. The upper limit is reached when penetration of the transmission line electric field into the plasma is limited by skin depth ($\sigma < 3 \times 10^{11}$ Hz for 30 MHz and a 1 cm radius plasma.)

20. DISTRIBUTION/AVAILABILITY OF ABSTRACT UNCLASSIFIED/UNLIMITED ☒ SAME AS RPT. ☐ OTIC USERS ☐	21. ABSTRACT SECURITY CLASSIFICATION UNCLASSIFIED
22a. NAME OF RESPONSIBLE INDIVIDUAL R. E. Pechacek	22b. TELEPHONE NUMBER (Include Area Code) (202) 767-2077 22c. OFFICE SYMBOL Code 4763

DD FORM 1473, 83 APR EDITION OF 1 JAN 73 IS OBSOLETE.

SECURITY CLASSIFICATION OF THIS PAGE

11. TITLE

A TRANSMISSION LINE BRIDGE FOR THE DIAGNOSTICS OF PLASMA CHANNELS

16. SUPPLEMENTARY NOTATION (Continued)

This research was supported by the Office of Naval Research and by the Defense Advanced Research Projects Agency (DoD) ARPA Order No. 4395, Amendment No. 11, monitored by the Naval Surface Weapons Center under Contract N60921-83-WR-W0014.

CONTENTS

A TRANSMISSION LINE BRIDGE FOR THE DIAGNOSTICS OF PLASMA CHANNELS

INTRODUCTION

This paper describes a device for measuring the average electrical conductivity of a long, narrow, cylindrical plasma. Interest in plasmas of this shape originates from two areas of study: the study of electron beam propagation through neutral gas, and the study of long straight electrical discharges for use as a communication antenna. Propagation of an electron beam through a neutral gas produces an ionized channel whose properties and evolution are very important to the propagation of the beam itself. Long straight electrical discharges are created in a channel that is ionized by a pulsed laser beam focused with a long focal length lens, and the properties of the plasma in this channel are important to the propagation of the electrical discharge along the channel. The properties of these plasmas are inferred from changes in the transmission properties of a transmission line placed close to and parallel to the plasma.

In ~~the following sections~~ this paper an analysis is made of the relation between the bridge output voltage and the conductivity of the perturbing plasma for the case in which the conductivity is very low. In this case all perturbations on the bridge parameters are small, and linear approximations are appropriate. The usefulness of the bridge, however, extends to plasma well above this low conductivity range, although a different set of approximations may be necessary to make the analysis of the experiment tractable.

DESCRIPTION OF TRANSMISSION LINE BRIDGE APPARATUS

A transmission line bridge is a device for measuring very small changes in the properties of transmission lines. If two identical lines are excited by identical signals, the two output signals are also identical. The difference between the two output signals is a null signal. A change in transmission of one of the lines results in a difference signal which may be made arbitrarily large by amplification with a high gain amplifer or by increasing the amplitude of the exciting signal. In practice, noise and lack of balancing precision limit the useful gain of the signal amplifier, but sensitivity may be increased indefinitely by increasing the excitation amplitude.

Manuscript approved December 21, 1983.

Figure 1 is a schematic diagram of the transmission line bridge. The plasma that is to be measured is created along the centerline of the active leg of the bridge. The construction and arrangement of the bridge is such as to make the two legs as nearly identical as possible. The conductors of the two-wire transmission lines are one meter long pieces of 3/4" (1.91 cm) OD copper tubing with centers separated by 2" (5.08 cm). This combination produces a 200 Ω line. The lines are driven by 50 Ω signals of the same relative phase from a magic-T through balanced-to-unbalanced (50 Ω-to-200 Ω) matching transformers. The output signals from the two lines are substracted in the second magic-T. Identical phase shifters and attenuators in each line permit a null over a reasonable range of oscillator frequencies in the absence of a plasma. Finally, the null signal is amplified by a large dynamic range amplifier and displayed on an oscilloscope. The commercial items used in the bridge are listed in Appendix I.

SIGNAL GENERATION BY PHASE SHIFT AND ATTENUATION

An atmospheric plasma is a lossy dielectric. When plasma is introduced into the vicinity of the active line, the line's output is attenuated and shifted in phase. In this case the signal generated by subtracting the reference line output from the active line output is no longer the null signal, but is given by Eq. (1).

$$\Delta V = V_0 \exp(-\gamma z)\cos((k_0+\Delta k)z-\omega t) - V_0\cos(k_0 z-\omega t), \qquad (1)$$

where ΔV is the difference signal, γ is the attenuation factor of the active line, Δk is the change in propagation factor of the active line, and $V_0\cos(k_0 z-\omega t)$ is the output of the reference line. This second term is also the output of the active line in the absence of plasma.

In the approximation, γz, $\Delta k z \ll 1$, the amplitude of the difference signal is given by Eq. (2).

$$\Delta V = V_0 \left((\gamma z)^2 + (\Delta k z)^2\right)^{1/2} = V_0 z \left(\gamma^2+\Delta k^2\right)^{1/2} \qquad (2)$$

In the experimental arrangement of Fig. 1, the output signal from the amplifier is rectified by a video detector. The resulting signal is

proportional to the amplitude of the bridge difference signal, which is just what is given by Eq. (2). The detected output is symmetrically dependent on attenuation and phase shift, insensitive to their signs, and more sensitive to the larger of the two parameters.

Equation (2) is the essential result of this section. The analogy is exact between the transmission line bridge in the arrangement of Fig. 1 and an optical interferometer arranged to measure fractional fringe shifts by placing an optical detector on a dark fringe in the interference pattern. If the detectors were placed in the gray region of the interference pattern, the 90° point between dark and light fringes, the interaction between attenuation and phase shift is even worse. In this case, in the same small change approximation as above, the amplitude of the output signal is given by Eq. (3)

$$\Delta V = \sqrt{2}\, V_0 z(\Delta k - \gamma) \qquad (3)$$

In the optical case, this inevitable interaction between phase shift and attenuation can be unfolded by using signals from two orthogonally placed photo-detectors. In the electrical case, this interaction can be eliminated by using signal limiters and linear detectors.

RELATION BETWEEN THE PHASE SHIFT AND THE ATTENUATION OF THE TRANSMISSION LINE SIGNALS AND THE CHANNEL DIELECTRIC CONSTANT, CONDUCTIVITY, AND GEOMETRY

The previous section was strictly an exercise in trigonometry: the difference between two cosine functions of slightly different amplitude and argument was manipulated until a suitably simple relation was found. In this section, these amplitude and argument differences are related to small changes in the dielectric constant of the dielectric surrounding the conductors of a transmission line.

A two conductor transmission line is characterized by an inductance per unit length, L, and a capacitance per unit length, C. This type of line transmits TEM waves with a propagation constant, $k = \omega\sqrt{(LC)}$, for a wave of frequency ω. C is the actual capacitiance per unit length between the two conductors that form the transmission line. This capacitance is a linear function of the dielectric constant of the material that surrounds the two conductors. If the dielectric constant is real everywhere, k is also real and

the wave propagates without attenuation. If the dielectric constant is complex, that is, if the surrounding material has a non-zero conductivity, k is complex, and the wave is attenuated as it travels along the line. In complex notation, the voltage at any point along the line is given by

$$V(z,t) = V_0 \, \mathrm{Re} \, \{\exp i(kz - \omega t)\} \, . \tag{4}$$

If k is set equal to $k_0+\Delta k+i\gamma$, where Δk and γ are real, Eq. (4) is expressed as follows,

$$V(z,t) = V_0 \exp(-\gamma z) \cos(k_0 z + \Delta k z - \omega t), \tag{5}$$

where the notation is the same as in Eq. (1). In the approximation that the change in the capacitance per unit length is very small compared to the line's vacuum dielectric capacitance per unit length the following equations relate the line's transmission parameters to the change in capacitance:

$$k = \omega (LC)^{1/2}$$

$$k = \omega (L_0 C_0 + L_0 \Delta C)^{1/2}$$

$$k = \omega (L_0 C_0)^{1/2} (1 + \Delta C/C_0)^{1/2} \tag{6}$$

$$k = k_0 (1 + \Delta C/C_0)^{1/2} \approx k_0 + (k_0/2C_0) (\mathrm{Re}(\Delta C) + i \mathrm{Im}(\Delta C))$$

$$k = k_0 + \Delta k + i\gamma$$

where $\Delta k = \dfrac{k_0}{2C_0} \mathrm{Re}(\Delta C)$ and $\gamma = \dfrac{k_0}{2C_0} \mathrm{Im}(\Delta C)$.

This (LC) analysis is valid only for TEM waves and lines that support them. If a change in the dielectric creates a condition in which TE or TM waves can propagate, the effect must be of second order for this analysis to be valid.

The capacitance of a transmission line is calculated by integrating the electric field energy density in the space between the conductors and then equating this value to $\frac{1}{2}CV^2$,

$$\frac{1}{2}CV^2 = \frac{1}{2}\int \varepsilon E^2 d^3r, \tag{7}$$

where V is the voltage difference across the conductors and ε is the dielectric constant. In general, ε is a function of position. Let ε_o be the dielectric constant of the reference line and the unperturbed active line, and let ε_r and ε_i be real and imaginary normalized perturbations on that dielectric constant $(\varepsilon = \varepsilon_o(1+\varepsilon_r+i\varepsilon_i))$. Then

$$C = \frac{1}{V^2}\int \varepsilon_o E^2 d^3r + \frac{1}{V^2}\int \varepsilon_r \varepsilon_o E^2 d^3r + \frac{1}{V^2}\int i\varepsilon_i \varepsilon_o E^2 d^3r$$

$$= C_o + \mathrm{Re}(\Delta C) + i\,\mathrm{Im}(\Delta C), \tag{8}$$

where $\varepsilon_r(r)$ and $\varepsilon_i(r)$ are in general functions of r, although uniform along the axis. E may be taken as the unperturbed field provided ε_i, $\varepsilon_r \ll 1$.

The main result of this section is the relationship between the attenuation constant and the change in propagation constant as a function of a perturbation in the transmission dielectric. This is achieved by combining Eq. (8) with Eq. (6):

$$\gamma = \frac{k_o}{2C_o V^2}\int \varepsilon_i \varepsilon_o E^2 d^3r\,, \tag{9}$$

$$\Delta k = \frac{k_o}{2V^2 C_o}\int \varepsilon_r \varepsilon_o E^2 d^3r\,.$$

By writing $\frac{1}{2}C_o V^2$ in Eq. (9) as the integral over the electrical stored energy in the transmission line, it becomes clear as shown in Eq. (10), that γ is proportional to the ratios of the energy loss per cycle to the total electric energy in the line and that Δk is proportional to the ratio of the perturbed stored energy to the total energy.

$$\gamma = \frac{k_o}{2} \frac{1/2 \int \varepsilon_i(r) \varepsilon_o E^2 d^3 r}{1/2 \int \varepsilon_o E^2 d^3 r}$$

$$\Delta k = \frac{k_o}{2} \frac{1/2 \int \varepsilon_r(r) \varepsilon_o E^2 d^3 r}{1/2 \int \varepsilon_o E^2 d^3 r} \qquad (10)$$

In Equations (10), γ and Δk are the experimentally measured quantities, and information about the plasma density and temperature is contained in $\varepsilon_r(r)$ and $\varepsilon_i(r)$. To solve these equations for $\varepsilon_r(r)$ and $\varepsilon_i(r)$, it is necessary to assume a spatial distribution for the plasma, that is, it is necessary to assume $\varepsilon_{r,i} = \alpha F(r)$ where $F(r)$ is assumed to be known and α is a constant to be found. The resulting expressions for $\varepsilon_r(r)$ and $\varepsilon_i(r)$are given in Equations (11):

$$\varepsilon_r(r) = \left(\frac{2\gamma}{k_o} \frac{1/2 \int \varepsilon_o E^2 d^3 r}{1/2 \int F(r) \varepsilon_o E^2 d^3 r}\right) F(r) \qquad (11)$$

$$\varepsilon_i(r) = \left(\frac{2\Delta k}{k_o} \frac{1/2 \int \varepsilon_o E^2 d^3 r}{1/2 \int F(r) \varepsilon_o E^2 d^3 r}\right) F(r)$$

In the right hand sides of Equations (11), Δk and γ are measured quantities, E is determined by the transmission line geometry and $F(r)$ is assumed.

APPLICATION TO A LASER PLASMA EXPERIMENT

The system of Fig. 1 has been used to measure the electron density produced by a long, Nd:glass-laser-produced spark in atmospheric pressure air and to measure the electron density produced by a CO_2 laser beam in 40T ammonia. The change in the dielectric, in each experiment, is due to an approximately 1 cm radius plasma that is created along the symmetry axis of a two wire transmission line. (See Fig. 2.) The solution for the potential outside two parallel, circularly cylindrical, equipotential, surfaces i.e., a two wire transmission line is given in Ref. 1. If it is assumed that the plasma cross section is circular, uniform, and centered on the transmission line axis, the integrals of Eq. (11) can be evaluated in terms of tabulated functions, provided that ε_r, ε_i are small enough such that the electric

field of Eq. (11) may be assumed to be the unperturbed fields of the transmission line. Because the plasma is uniform for $r<r_o$, and doesn't extend beyond $r=r_o$ the integrals for the perturbed energy in Eq. (11) become

$$\tfrac{1}{2}\int_{\text{all space}} \varepsilon_{r,i}(r)\,\varepsilon_o E^2(r)\,d^3r = \tfrac{1}{2}\,\varepsilon_{r,i}\int_{\text{plasma } (r<r_o)} \varepsilon_o E^2(r)\,d^3r \quad . \tag{12}$$

The expression for the imaginary and real parts of the perturbation of the dielectric constant is then

$$\varepsilon_i = \frac{2\gamma}{k_o}\,\frac{\tfrac{1}{2}\int_{\text{all space}} \varepsilon_o E^2 d^3r}{\tfrac{1}{2}\int_{r<r_o} \varepsilon_o E^2 d^3r} = \frac{\gamma}{k_o}\,\frac{1}{B(d/s)A(r_o/\delta)}\,, \tag{13}$$

$$\varepsilon_r = \frac{\Delta k}{k_o}\,\frac{1}{B(d/s)A(r_o/\delta)}\,,$$

where d is the diameter of the transmission line conductors, s is their separation, δ is equal to $\frac{1}{2}\sqrt{(S^2-d^2)}$, and r_o is the radius of the plasma column. These lengths are shown schematically in Figure 2.

The value of the integral in the numerator, the total electrostatic energy of a two wire transmission line, is a function of the ratio d/s. The integral in the denominator, is proportional to the product of a function of d/s and a function of r_o/δ . It follows that the ratio of the two integrals can be represented as the product of two independent functions, B(d/s) and $A(r_o/\delta)$ in Equation (13). The expressions for A and B are as follows:

$$A(\alpha) = \ln\left(\frac{1+\alpha^2}{1-\alpha^2}\right)\,, \quad \alpha<1$$

$$B(\alpha) = \frac{\ln\left((1+\sqrt{1-\alpha^2})/\alpha\right)}{\left(\ln\dfrac{1+\sqrt{1-\alpha^2}}{1-\sqrt{1-\alpha^2}}\right)^2} \quad \alpha<1, \tag{14}$$

and they are plotted in Fig. 3.

For the 200 Ω line of Fig. 2, d/s = .375, δ = 2.35 cm, and r_o/δ = .4, which results in $A(r_o/\delta) = 0.32$ and $B(d/s) = 0.16$. The frequency used in the bridge of Fig. 1 is 30 MHz which corresponds to $k_o = .628\ m^{-1}$. The relation between the bridge output voltage and the dielectric change is obtained from Equation (2) and Equation (13):

$$\Delta V = zk_o AB(\varepsilon_i^2 + \varepsilon_r^2)^{1/2} V_o = .032(\varepsilon_i^2 + \varepsilon_r^2)^{1/2} V_o \qquad (15)$$

Both of these experiments were operated at high enough pressures (1 atm and 40T) and low enough driving frequency, ω, such that $\upsilon >> \omega_p >> \omega$, where υ is the electron-neutral collision frequency, and ω_p is the plasma frequency. The result is that $\varepsilon_r^2 << \varepsilon_i^2$, and

$$\varepsilon_i = (.032)^{-1} \frac{\Delta V}{V_o} = 30.1\ \Delta V/V_o \qquad (16)$$

The lower limit of usefulness of this expression is that the signal must be significantly larger than amplifier noise: $\Delta v > 10^{-5}$ volts. On the upper end, γ/k_o must be small enough that the linear approximations of Eq. (6) are valid: $\gamma/k_o < 0.1$; also, ε_i must be small enough for the use of the unperturbed fields in Eq. (13) to be valid. The requirement on ε_i includes the requirement on γ/k_o. These limits are

$$0.2 > \varepsilon_i > \frac{3.2\times10^{-4}}{V_o} = \Delta V_{min}/.032\ V_o. \qquad (17)$$

In cgs units $\varepsilon_i = 4\pi\sigma/\omega$ (σ is the conductivity) and the limits on σ are

$$1.5\times10^{6} > \sigma > \frac{4.8\times10^{3}}{V_o} \qquad (18)$$

In the attempts to measure the conductivity of a CO_2 laser produced channel in 40T NH_3 the value of V_o was set at 2 volts. No measurable signal was detected, which implies that $\sigma < 2.4\times10^3$ Hertz ($n_e < 5\times10^5\ cm^{-3}$).

In the Nd/Glass laser spark in atmospheric air experiment, the Nd/Glass laser is focussed along the axis of the the active leg of the transmission line bridge. An open shutter photograph of the resulting one meter long plasma is shown in Figure 4. The bridge output (for V_o=.16 volts, rms) produced by this plasma, after the signal has been amplified by a logarithmic

amplifier and rectified by a video detector, is shown in the oscilloscope photograph in Figure 5. The plasma conductivity is determined from this video output signal by taking its antilogarithm and multiplying by an appropriate constant. This result is shown in Figure 6, a plot of the plasma conductivity versus time. The plasma has a peak conductivity of 1.4×10^6Hz which decays to zero in about 300 μsec .

REMARKS ON SENSITIVITY AND APPROXIMATIONS

The inherent limitations of a transmission line bridge as a plasma diagnostic are spatial limitations: (1) the attenuation constant measured by the bridge is the average attenuation constant along the entire length of the line. The same limitation applies to the measurement of the change in propagation constant. If the plasma is axially uniform the measurement is exact. However, the degree of axial uniformity must be determined from other measurements. (2) A radial profile of the plasma also based on other measurements must be assumed. The reason for this is that many different distributions of dielectric material can produce the same change in propagation constant.

Three restrictions or assumptions are made in the analysis in the preceding sections that take advantage of the fact that the plasma of interest has a very low conductivity:

$$\gamma z,\ \Delta k z \ll 1,$$

$$\gamma / k_0,\ \Delta k / k_0 = \Delta C / C_0 \ll 1$$

$$\varepsilon_i,\ \varepsilon_r \ll 1 \quad .$$

If these restrictions are relaxed, the bridge is able to diagnose plasmas of much higher conductivity although the analysis is no longer as straightforward.

The first restriction can be removed by a change in the hardware: by replacing the simple network (magic T), that takes the difference between the reference arm and the active arm signals, with a pair of balanced mixers operating 90° out of phase with one another. A balanced mixer is a device that produces the average value of the product of two signals. These mixers

would produce output signals that correspond to Eq. (1), and would allow γ and Δk to be separated for all values of Δkz and γz:

$$\Delta V_1 = V_o e^{-\gamma z} \cos \Delta kz$$
$$\Delta V_2 = V_o e^{-\gamma z} \sin \Delta' \gamma \quad . \tag{19}$$

Since γ, Δk and Δv are no longer linearly related, an extra step is involved in the data analysis. The solution of these equations for γ and Δk are

$$\Delta k = \frac{1}{z} \tan^{-1} \frac{\Delta V_2}{\Delta V_1}$$
$$\gamma = \frac{-1}{2z} \ln \left(\left(\frac{\Delta V_1}{V_o}\right)^2 + \left(\frac{\Delta V_2}{V_o}\right)^2 \right) \quad . \tag{20}$$

The second restriction of the experimental data analysis can always be met by making the transmission line cross sections very large compared to the cross section of the plasma. If the plasma is so comparatively small that it intercepts only 10% of the transmission line's electrostatic energy then $\left|\Delta C/C_o\right| = \left|\frac{i\gamma + \Delta k}{2k_o}\right| < .1$ and the condition is satisfied. If this restriction cannot be met, an added complexity must be handled in relating the measured γ and Δk to the change in capacity per unit length:

$$\frac{i\gamma + \Delta k}{k_o} = \sqrt{1 + \frac{\Delta C}{C_o}} - 1 \quad . \tag{21}$$

Thus, the second restriction, like the first, is made to facilitate the analysis of the measurements and does not represent a limit on the conductivity range of usefulness of the bridge.

The final restriction, ε_i, $\varepsilon_r \ll 1$, is the most serious. It comes about because of the ease of computation that is the result of assuming that the electric field in the plasma is the same as the vacuum or unperturbed field. Large values of ε_i or ε_r may be handled without an exact solution of the boundary value problem if the diameter of the plasma, relative to the

transmission line, is small enough such that the following approximation is valid: the unperturbed electric field within the volume of the plasma is a constant. In this case the solution to the problem of a dielectric rod immersed in a uniform electric field applies, and the field inside the rod, E, as a function of the external field, E_0, is uniform and given by

$$E = \frac{2E_0}{1 + \left((1+\varepsilon_r)^2+\varepsilon_i^2\right)^{1/2}} \qquad (22)$$

where ε is the perturbation of the dielectric constant. Thus the limit on ε in this high conductivity case is that the skin depth of the plasma be large compared to the plasma radius, so that the field inside the plasma is uniform. For a collisionally dominated plasma, this condition is

$$r_0^2 \ll c^2/2\pi\sigma\omega \quad ,$$

which implies a maximum σ of 3×10^{11} Hz for 30 MHz excitation and r_0 = 1 cm. For a collisionless plasma, the plasma frequency must be less than the applied frequency for the applied field to penetrate the plasma.

The input noise of the bridge amplifier determines the ultimate sensitivity of the system. This noise can be reduced by reducing the bandwidth of the amplifier: system sensitivity is directly exchangeable for response time. If V_n is the noise voltage of the amplifier input, $(\gamma z)_{min}$ or $(\Delta kz)_{min}$, the minimum detectable signals are equal to V_n/V_0, where V_0 is the transmission line voltage. The minimum detectable signal can also be reduced by increasing V_0.

In an optical interferometer, if the length of the two optical paths are made equal, variations in source wavelength do not significantly affect the output. Similarly, if the phase shift and attenuation of the arms of the transmission line bridge are made equal, oscillator noise is eliminated from the bridge output.

EXAMPLE OF AN ANALYSIS OF A HIGH CONDUCTIVITY PLASMA MEASUREMENT

An interesting example is the case of a very narrow, highly conductive, uniform plasma in a two-wire transmission line bridge. The relation between the transmission line's attenuation constant and the imaginary part of the

perturbation on the vacuum dielectric constant, $\varepsilon_i = 4\pi\sigma/\omega$, is analysed below for the case in which $\varepsilon_i \approx 1$, $\varepsilon_r << \varepsilon_i$, $r_o << \delta$ (δ is defined in Fig. 2), and $\gamma << k_o$. Equation (11) is a statement of this relationship. F(r) is set equal to one since the plasma is assumed to be uniform. The integral in the numerator of Eq. (11) is the total electrostatic energy in the line and is equal to $\pi V^2[2 \cosh^{-1} (s/d)]^{-1}$. To evaluate the integral in the denominator the component of the electric field near the symmetry axis of the two wire transmission line is computed from reference (1):

$$E_o = \frac{2V}{\delta(1-x^2/\delta^2)\ln(\frac{s+2\delta}{2-2\delta})} \approx \frac{2V/\delta}{\ln(\frac{s+2\delta}{s-2\delta})} \quad . \tag{23}$$

The relationship between ε_i and γ is obtained by substituting Eqs. (22) and (23) into Eq. (11):

$$\varepsilon_i = \frac{\gamma}{2k_o} \left(\frac{1+\sqrt{1+\varepsilon_i^2}}{2}\right) \frac{\delta^2}{r_o^2} \frac{\ln^2(\frac{s+2\delta}{s-2\delta})}{\cosh^{-1} s/d} \quad . \tag{24}$$

CONCLUSIONS

The transmission line bridge, when used at 30 MHz and as configured in Fig. 1, is capable of measuring the time evolution of plasma channel conductivity for a channel in high pressure gas. (Electron-neutral collisions dominate the plasma.) The bandwidth of the system is about 4 MHz, and the largest source of error is the estimate of the plasma geometry. Operating the bridge at different frequencies or creating the plasma at different gas pressures will yield different relations between ε_r and ε_i than the particularly simple one for the cases cited here: $\varepsilon_r << \varepsilon_i$. In general, it is necessary to measure two quadrature outputs to unravel ε_r and ε_i.

ACKNOWLEDGMENTS

The authors are indebted to Y.Y. Lau for pointing out that the solution to La Place's equation for two-wire transmission line is contained in Ref. 1. They are also grateful for the technical assistance of E. Laikin and S. Hauver.

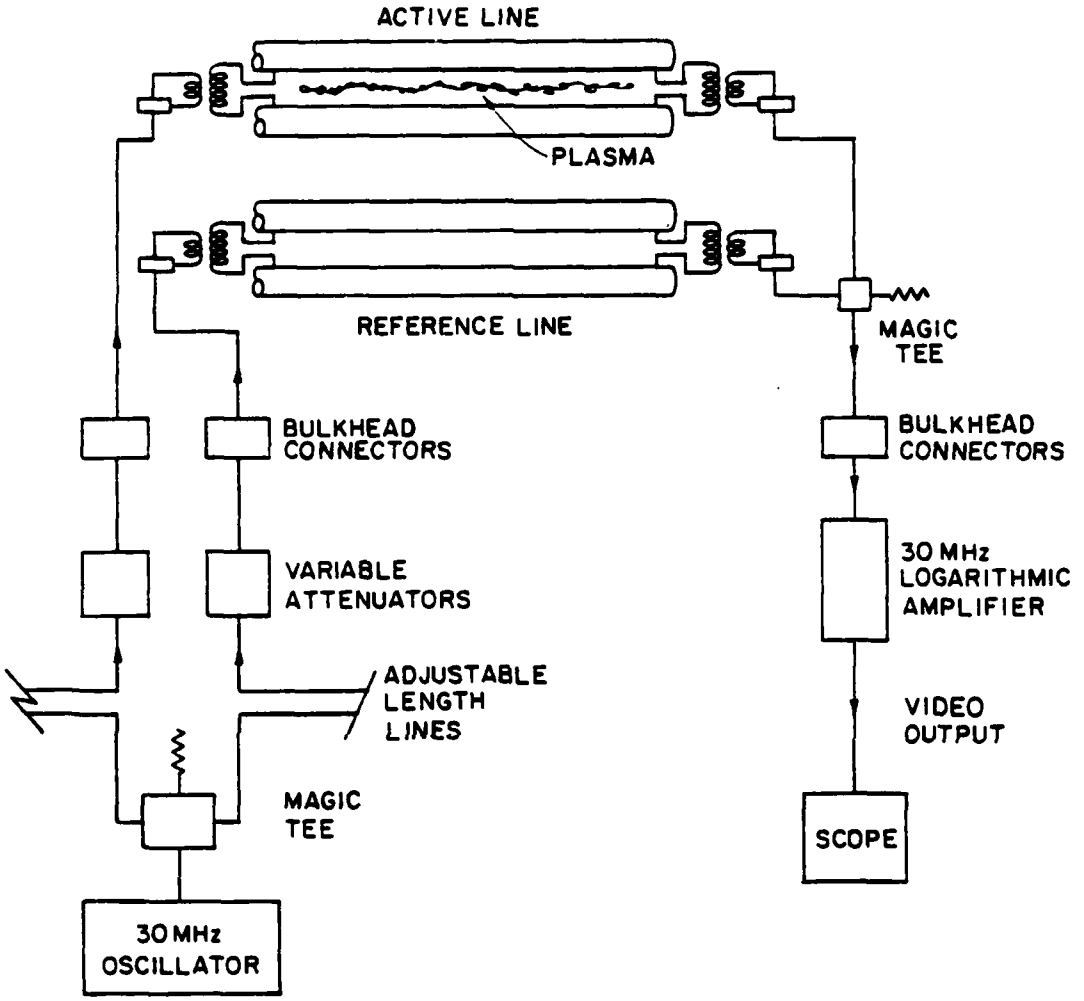

Figure 1. A schematic diagram of the transmission line bridge.

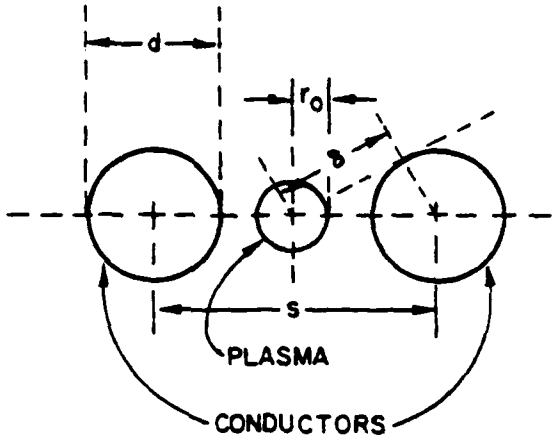

Figure 2. Cross section of the active leg of the transmission line bridge.

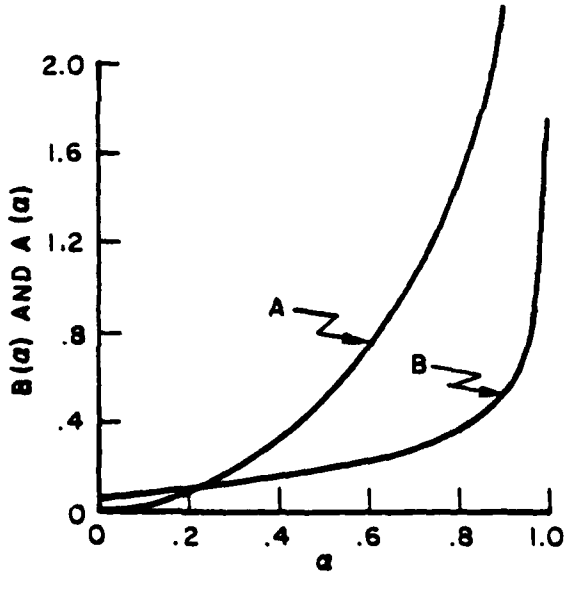

Figure 3. A plot of the functions A(α) and B(α), whose product, for appropriate α's, is one half of the ratio of the perturbed to total electrostatic energy in a two-wire transmission line perturbed by a dielectric rod along its axis.

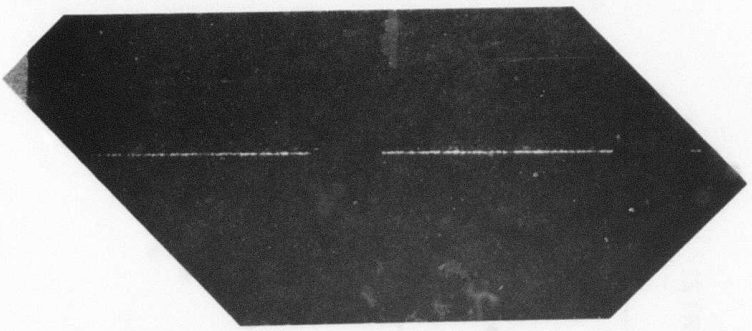

Figure 4. Still camera photograph of a one meter long plasma produced by a focused Nd:glass laser. The gap in the center is caused by an obstruction in front of the camera.

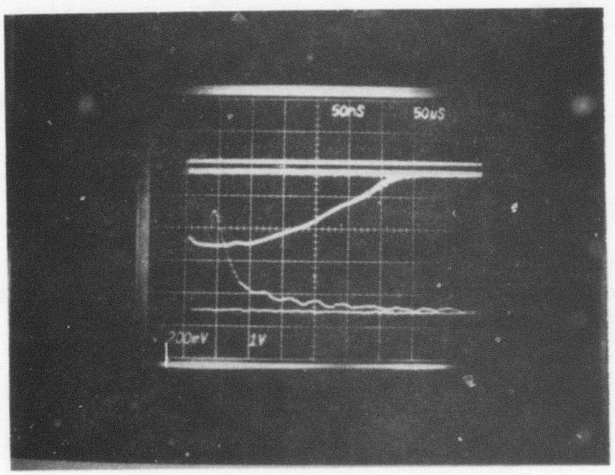

Figure 5. Oscilloscope photograph of the log-amplified output of the transmission line bridge. The top line is the zero voltage line. The second line is the amplifier noise output. The third line is the bridge signal caused by the Nd:glass laser plasma. The oscilloscope gain is 200 mv/div and the sweep speed is 50 µsec/div. The lower two traces are the laser output pulse and a baseline at 1 v and 50 nsec per division.

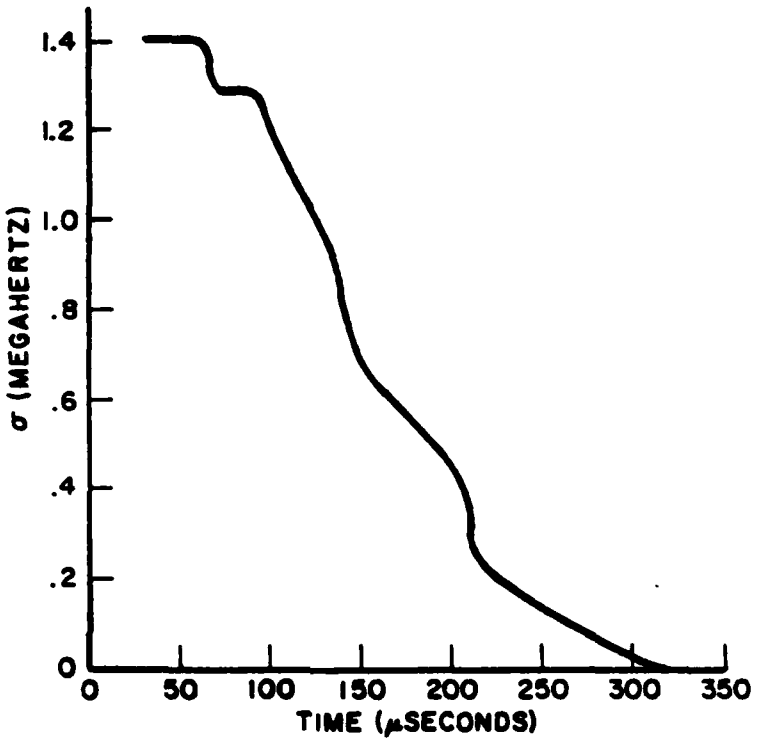

Figure 6. Conductivity as a function or time of the Nd:glass laser produced plasma in atmospheric pressure air. The conductivity is computed from a transmission line bridge measurement.

REFERENCES

1. Carrier, G. R., Crook, M. and Pearson, C. E., "Functions of the Complex Variable," McGraw Hill, New York, 1966, p. 129.

APPENDIX I - PARTS LIST

The list of components used in the transmission line bridge circuit and shown schematically in Fig. 1 is as follows:

50 Ohm, unbalanced, to 200 Ohm, balanced, transformer - Anzac Electronics, Waltham, MA, Model TP-104.

50 Ohm Magic Tee - Anzac Electronics, Waltham, MA, Model HH-107.

Phase Shifter - General Radio Company, Concord, MA, Type 874-LTL.

Attenuator - Mini-Circuits Laboratory, New York, NY, Model ZAS-3B.

Oscillator - Hewlett-Packard Company, Palo Alto, CA, Model 8640B.

DISTRIBUTION LIST

1. Dept. of the Navy
   Chief of Naval Operations
   Washington, D.C. 20350
   ATTN: Dr. C. F. Sharn (op 987)

2. Commander
   Naval Sea Systems Command
   Department of the Navy
   Washington, DC 20363
   ATTN: NAVSEA/PMS 405 (Dr. Finkleman)

3. Air Force Weapons Laboratory (NTYP)
   Kirtland Air Force Base
   Albuquerque, New Mexico 87117
   ATTN: Maj. James Head
   Dr. David Straw

4. U.S. Army Ballistics Research Laboratory
   Aberdeen Proving Ground, Maryland 21005
   ATTN: Dr. D. Eccleshall (DRDAR-BLB)

5. Ballistic Missile Defense Advanced Technology Center
   P. O. Box 1500
   Huntsville, Alabama 35807
   ATTN: Dr. L. Harvard (BMDSATC-1)

6. B-K Dynamics Inc.
   15825 Shady Grove Road
   Rockville, Maryland 20850
   ATTN: Dr. R. Linz

7. Lawrence Livermore Laboratory
   University of California
   Livermore, California 94550
   ATTN: Dr. R. J. Briggs
   Dr. T. Fessenden
   Dr. W. Barletta
   Dr. D. Prono

8. Mission Research Corporation
   735 State Street
   Santa Barbara, California 93102
   ATTN: Dr. C. Longmire
   Dr. N. Carron

9. Pulse Sciences Inc.
Suite 610
1615 Broadway
Oakland, California 94612
ATTN: Dr. S. Putnam

10. Science Applications, Inc.
Security Office
5 Palo Alto Square, Suite 200
Palo Alto, California 94304
ATTN: Dr. R. R. Johnston
Dr. Leon Feinstein

11. Naval Surface Weapons Center
White Oak Laboratory
Silver Spring, Maryland 20910
ATTN: Mr. R. J. Biegalski
Dr. R. Cawley
Dr. J. W. Forbes
Dr. C. M. Huddleston
Dr. H. S. Uhm
Dr. R. B. Fiorito

12. C. S. Draper Laboratories
555 Technology Square
Cambridge, Massachusetts 02139
ATTN: Mr. E. Olsson

13. Physical Dynamics, Inc.
P. O. Box 1883
LaJolla, California 92038
ATTN: Dr. K. Brueckner

14. Office of Naval Research
Department of the Navy
Arlington, Virginia 22217
ATTN: Dr. W. J. Condell (Code 421)

15. Avco Everett Research Laboratory
2385 Revere Beach Pkwy.
Everett, Massachusetts 02149
ATTN: Dr. R. Patrick
Dr. Dennis Reilly

16. Defense Technical Information Center
Cameron Station
5010 Duke Street
Alexandria, Virginia 22314 (2 copies)

17. Naval Research Laboratory
Washington, D. C. 20375
ATTN: T. Coffey - Code 1001
M. Lampe - Code 4792
M. Friedman - Code 4700.1
J. R. Greig - Code 4763 (50 copies)
I. M. Vitkovitsky - Code 4701
W. R. Ellis - Code 4000
S. Ossakow, Supt. - 4700 (26 copies)
Library - Code 2628 (20 copies)
A. Ali - Code 4700.1T
D. Book - Code 4040
J. Boris - Code 4040
S. Kainer - Code 4790
A. Robson - Code 4760
M. Picone - Code 4040
M. Raleigh - Code 4763
R. Pechacek - Code 4763
J. D. Sethian - Code 4762
K. A. Gerber - Code 4762
G. Joyce - Code 4790
D. Colombant - Code 4790
B. Hui - Code 4790

18. Defense Advanced Research Projects Agency
1400 Wilson Blvd.
Arlington, Virginia 22209
ATTN: Dr. J. Mangano
Lt. Col. R.L. Gullickson

19. JAYCOR
205 S. Whiting St.
Alexandria, Virginia 22304
ATTN: Dr. R. Hubbard
Dr. R. Fernsler

20. Mission Research Corp.
1720 Randolph Road, S. E.
Albuquerque, New Mexico 87106
ATTN: Dr. Brendan Godfrey

21. Princeton University
Plasma Physics Laboratory
Princeton, New Jersey 08540
ATTN: Dr. F. Perkins, Jr.

22. McDonnell Douglas Research Laboratories
Dept. 223, Bldg. 33, Level 45
Box 516
St. Louis, Missouri 63166
ATTN: Dr. Michael Greenspan
Dr. J. C. Leader

23. Cornell University
Ithaca, New York 14853
ATTN: Prof. David Hammer

24. Sandia Laboratories
Albuquerque, New Mexico 87185
ATTN: Dr. Bruce Miller, 4255
Dr. Carl Ekdahl
Dr. M. Mazarakis

25. Naval Air Systems Command
Washington, D. C. 20361
ATTN: Dr. J. Reif, Code AIR-350F

26. Beers Associates, Inc.
P. O. Box 2549
Reston, Virginia 22090
ATTN: Dr. Douglas Strickland

27. U. S. Department of Energy
Washington, D. C. 20545
Office of Fusion Energy, ATTN: Dr. W. F. Dove
Office of Inertial Fusion, ATTN: Dr. Richard L. Schriever

Director
U.S. Department of Energy
ER20:GTN, High Energy and Nuclear Physics
Attn: Dr. T. Godlove
Washington, DC 20545

28. AFOSR/NP
Bolling Air Force Base, Bldg. 410
Washington, D. C. 20331
ATTN: Capt. H. Pugh

29. Foreign Technology Division
Wright Patterson AFB, OH 45433
ATTN: Mr. C. J. Butler/TQTD

30. Aerospace Corp.
P. O. Box 92957
Los Angeles, CA 90009
ATTN: Dr. A. Christiansen A6/2407
Dr. E. Frazier

31. SRI International
333 Ravenswood Avenue
Menlo Park, CA 94025
ATTN: Dr. D. Eckstrom

32. Los Alamos National Laboratory
Los Alamos, NM. 87545
ATTN: Dr. T. P. Starke, M-2

33. G T Devices
5705 General Washington Drive
Alexandria, VA 22312
ATTN: Dr. D. A. Tidman
Dr. S. A. Goldstein